NERTHUS: NEutRon THermal time-focUssing Spectrometer

Marco Zanatta (University of Trento, Italy);
Mohamed Aouane, Christian Balz, and Daria Noferini (ESS, Sweden);
Andrea Orecchini and Francesco Sacchetti (University of Perugia, Italy).

1 EXECUTIVE SUMMARY

NERTHUS is a spectrometer optimised for neutron Brillouin scattering (NBS) in combination with polarisation analysis and generalised density of states (GDOS) measurements. NBS consists in measuring the dispersion curves and lifetimes of coherent collective excitations in non-crystalline samples, either solid or liquid, where propagating modes can be detected only within the first (pseudo-) Brillouin zone. There exists a host of science cases that can greatly benefit from this, or can only be tackled in this way, for which NERTHUS will unlock unique possibilities.

To give a few examples, in the field of life sciences, pharmaceutics and drug design, NERTHUS will allow a comprehensive characterisation of the coherent dynamics in biomacromolecules, such as proteins, enzymes or nucleic acids, where collective modes are known to play an important role for biological function. For energy-related materials, NERTHUS will shed new light on the coupling between lattice vibrations and transport properties in functional materials.In magnetism, it will probe low-Q ferromagnetic excitations in powders and 2D magnets, revealing the microscopic magnetic interactions critical for quantum devices, spintronics, and novel magnetic materials.

The technique of NBS involves thermal or higher exchanged energies E in combination with wavevector transfers Q down to 0.1 Å^{-1}. An efficient access to this specific (Q, E) region with a neutron spectrometer is intrinsically difficult and requires specific technical characteristics: namely thermal and hot incident energies, small-angle detection, low beam divergence, low background, obviously with the highest possible incident flux. Combining together all these characteristics in a general purpose spectrometer turns out to be inefficient. Indeed, previous or existing instruments, devoted to general science cases and offering NBS as a special configuration only, have often underperformed. On the other hand, the only dedicated instrument ever existed (BRISP at the ILL) suffered from an intrinsically high background due to its unfortunate location on the only available, but sub-optimal, beamport. One of the main shortcomings of NBS arises from the fact that "traditional" spectrometers tend to relax beam divergence to increase flux, which does not severely impact the Q-resolution at wide and intermediate scattering angles. On the other hand, a strictly controlled and clean divergence is essential for an NBS measurement, but reduces flux by almost an order of magnitude on traditional spectrometers.

Here we proposed the use of a double time-focusing crystal monochromator which, in combination with the unique long pulse of ESS, allows the preparation of an unprecedentedly clean incident beam, with low divergence and no direct sight to the source, without trading off incident flux. The marked displacement of the sample position from the source line-of-sight, resulting from the double reflection at the monochromator, frees up the room for an easy installation of polarisation analysis equipment, which has nowadays become of multidisciplinary interest, and wide angle detector banks, which can supplement NBS with the traditional dynamical range and complementary GDOS measurements.

Analytical calculations, ray-tracing simulations and past prototype tests of the double focusing monochromator promise a flux gain of more than an order of magnitude with respect to presently planned ESS thermal spectrometers, without any significant background increase. Nowadays, the availability of TBL at ESS could be exploited for a further fine-tuning of the double monochromator onto the specific shape of the ESS neutron pulse.

2 SCIENTIFIC CASE

2.1 Key scientific drivers

2.1.1 Disordered materials and liquids

Disordered materials constitute a broad class of systems characterised by the presence of topological disorder, i.e. the absence of crystal-like long-range order. Disordered materials include liquids, supercooled liquids, glasses, polymers, and colloids. Biological systems such as proteins, DNA, cells, and even tissues belong to the same class of systems.

Collective dynamics of disordered systems and liquids. In the macroscopic regime, when the wavelength of an external probe is much larger than the typical interatomic spacing, network details can be neglected and disordered materials support sound waves similarly to powdered crystals. Decreasing the length scale to a few nanometers, the continuum approximation breaks down,

and acoustic excitations evolve towards a more complex pattern of vibrations characterised by damped, phonon-like excitations. The study of these features requires a wide kinematic range and high resolution in both E and Q. Recent results on glasses and liquids have shown a pattern of collective modes with a complexity higher than previously expected, e.g. [1, 2]. Nowadays, this domain is accessible only by inelastic X-ray scattering (IXS) at major synchrotron facilities. However, compared to X-rays, neutrons are more sensitive to hydrogen and low-Z elements, whose detection is fundamental in the study of water and molecular liquids. At the same time, neutrons can be effectively used to study high-Z liquid metals [3]. Being optimised for Brillouin neutron scattering, NERTHUS will boost these studies. The high flux will allow for the investigation of small samples with complex sample environments. Moreover, NERTHUS will offer the possibility of measuring collective excitations and the density of states at the same time. Their quantitative comparison was recently identified as a potential way to determine the longitudinal and transverse nature of the modes, see Ref. [2].

Vibrational dynamics in disordered systems. Despite the large spectrum of different chemical and physical properties, disordered materials exhibit universal vibrational features that are intimately related to their disordered structure. A well-known example is the boson peak, a broad peak visible in the low-energy region (a few meV) of the reduced vibrational density of states $g(E)/E^2$ of disordered systems. This intriguing feature is universally visible in the same energy domain, and its origin is still a debated topic [4]. The wide E_i range, the small Q, and the variable resolution will enable measurements of $g(E)$ over a wide E range, even for coherent samples, through a proper extrapolation towards the incoherent approximation. NERTHUS will thus provide an effective tool for gathering information on the nature of the vibrational density of states and the boson peak by studying its evolution as a function of pressure and temperature. Finally, recent works have highlighted the possibility of producing glasses via thermal vapor deposition, e.g. [5]. These glasses are named ultrastable glasses (USG) and show unique physicochemical properties: high thermal stability, improved mechanical properties, and anomalous transitions into the supercooled liquid, with great potential for the development of new applications, e.g. [6] and for understanding key aspects of the glassy state [7]. Typical USGs are produced from organic, H-rich materials that are perfect for inelastic neutron scattering studies and require the possibility of measuring both the vibrational density of states and the pattern of collective excitations.

2.1.2 Energy materials

Our society is more and more energy-intensive, hence increasing the demand for new energy storage and conversion technologies. As a result, a broad research effort spanning diverse energy sectors is driving the development of next-generation functional materials. Here we outline some examples where NERTHUS can offer new capabilities by providing access to the first (pseudo-) Brillouin zone, with the additional possibility to discriminate between incoherent scattering and coherent (plus isotope incoherent) scattering given by polarisation analysis. NERTHUS will enable measurements in energy ranges which are not covered or suffer from severe flux limitations on TREX, hence serving as an excellent complementary instrument with respect to TREX and CSPEC. Moreover, thanks to the large detector option, NERTHUS can also provide additional capacity to TREX in the overlapping kinematic range, especially for those experiments which would profit from the enhanced signal-to-noise ratio.

Superionic conductors for solid state batteries. While lithium-ion batteries remain the dominant technology, the safety limitations associated with liquid electrolytes and the demand for higher energy densities are driving the development of all-solid-state batteries. In such next-generation devices, superionic conductors (e.g., thiophosphates or garnet-type electrolytes) enable the replacement of flammable liquid electrolytes with solid materials that can offer improved safety, higher energy density, and enhanced electrochemical stability [8–13]. Their exceptional ionic conductivity arises from a strong coupling between mobile ions and the host-lattice dynamics: the ions exhibit liquid-like diffusivities within a largely ordered framework, facilitated by soft, anharmonic lattice vibrations and large-amplitude local modes that generate transient diffusion pathways and lower migration barriers [9, 14–21]. Understanding and controlling the lattice dynamics is thus essential for the development of all-solid-state batteries [12, 13, 16]. Many modern superionic conductors, particularly battery-relevant sulfide and halide electrolytes, are chemically complex and/or metastable. As a result, they are often available only as polycrystalline powders rather than large single crystals, complicating the resolution of low-Q acoustic phonon branches in scattering experiments [14, 15, 20–22]. By providing access to the first Brillouin zone for these materials, NERTHUS can more clearly elucidate the lattice dynamics that govern ion transport and ultimately the performance in applications.

Molten salts and liquid metals for solar, nuclear, and electrochemical technologies. Molten salts and liquid metals are pivotal in high-temperature energy systems, serving as efficient thermal energy storage media for concentrated solar power, high-capacity electrolytes and electrodes in grid-scale batteries, and advanced coolants for Generation IV nuclear reactors, as well as being integral to many fusion reactor concepts [23–30]. The high-frequency density fluctuations and phonon-like modes play a key role in determining the microscopic contributions to the thermal conductivity and viscosity, which are critical for the heat transfer efficiency and safety margins of reactor coolants, as well as in providing fundamental insights into the ion transport mechanisms

and the liquid-layer stability required for the operation of high-rate batteries [25, 31–33]. A detailed understanding of these collective excitations—an evergreen topic for thermal spectroscopy in general and NBS in particular—could strongly benefit from the enhanced capabilities of NERTHUS [33–36]. Such improved knowledge on these materials would provide valuable experimental benchmark for theory and simulations and support the optimisation of coolant and electrolyte compositions [25, 31].

Thermoelectric materials for waste heat recovery. Thermoelectric materials are increasingly explored as tools to recover the large fraction of energy dissipated as waste heat in industrial and transportation processes, by directly converting temperature differences into electrical power [37–39]. High performance is often interpreted in terms of the phonon-glass electron-crystal (PGEC) paradigm, in which crystalline electronic transport coexists with strongly suppressed, glass-like lattice thermal conductivity (κ) [37, 38, 40]. Cage-type compounds such as skutterudites and inorganic clathrates exemplify this concept: heavy, weakly bound "rattler" atoms are encapsulated in rigid frameworks, and their localized vibrations scatter heat-carrying acoustic phonons, driving κ towards low, weakly temperature-dependent values [37, 38, 41]. Inelastic neutron scattering experiments across a broad class of thermoelectrics, in cage and non-cage systems, revealed that this coupling often appears as an avoided crossing between flat rattling modes and acoustic branches, which is closely linked to reduced group velocities and enhanced phonon scattering [39, 41–44]. Because complex, heavily alloyed or disordered thermoelectrics exhibit crowded and broadened phonon spectra, a careful selection of the reciprocal-space regions, often near first-zone high-symmetry directions, is required to unambiguously resolve these features [39]. In addition, diffuse scattering arising from chemical disorder and incoherent background can mask the weak coherent phonon signals, complicating a reliable extraction of the phonon lifetimes. The use of polarisation analysis combined with the kinematic range of NERTHUS is therefore particularly valuable for isolating phonon modes from background and quantifying resonant rattler–acoustic interactions that suppress lattice thermal conductivity in PGEC-like materials [39].

Hydrogenated materials for solid-state fuel cells and solid-state storage. The progress of the hydrogen economy depends on high-performance solid-state storage (e.g., metal hydrides) and electrochemical conversion (e.g., proton-conducting fuel cells). In these materials, the functional performance is governed by the interplay between hydrogen dynamics—both individual proton hopping and collective vibrations of the hydrogen sublattice—and the lattice vibrations of the host structure [45–48]. In many hydrides and proton conductors, the acoustic phonons of the host are concentrated below a few tens of meV, whereas the hydrogen-related optical modes and H–H correlations may extend to several tens and beyond 100 meV [49, 50]. NERTHUS can capture the low-angle onset of these dispersions, cleanly resolving the long-wavelength acoustic modes from more localized hydrogen excitations over a broad energy range. Moreover, polarisation analysis would allow to isolate the underlying coherent excitations of both the host and the hydrogen from the dominant incoherent signal of the hydrogen self-dynamics, which typically masks the framework dynamics [51]. With this combination, NERTHUS will enable a quantitatively consistent picture of proton–lattice coupling and hydrogen self-dynamics.

2.1.3 Life Science and Pharmaceutics

Proteins, enzymes, DNA, RNA, lipid membranes are all central to cellular function. The static structures of these biomolecules are often known in great detail, but their functionality is crucially governed by their dynamical character too. Most vital molecular processes can only take place through structural changes of the involved proteins, enzymes or macromolecules. The molecular and atomic movements driving such structural changes are usually triggered by temperature and are often coupled, or even controlled, by the biological environment of the protein, such as hydration water or more complex physiological environments. In the latter respect, great interest is raised by the effects on protein dynamics of cryoprotectant moieties, like glycerol or trehalose, that can either plasticise or stabilise protein motions, thus resulting respectively in a faster reaction rate or in an increased protein stability, at a given temperature. Besides the obvious importance of understanding the fundamental mechanisms at the basis of biomolecular functions, this has strong impacts in the field of pharmaceuticals and drug design, because optimisation of the protein environment can control both drug delivery and drug shelf life.

As a consequence, there exists an overwhelming scientific literature on the diffusive and relaxational (incoherent) dynamics – occurring at pico- and nanosecond timescales – of proteins, nucleic acids, their hydration water or more complex environments. More recently, it has become clear that coherent collective dynamics can also play a crucial role in governing biological functions. For instance, both optical Kerr effect spectroscopy [52] and orientation-sensitive near-field microscopy [53] have independently revealed that THz vibrations (1-50 meV scale) propagating in specific directions of the lysozyme protein are involved in its functional ligand-binding process. Very recently, a revisited way of using normal mode analysis confirmed the important role played by coherent collective vibrations in protein conformational transitions [54]. A comprehensive characterisation of collective modes in biomacromolecules has therefore become of undoubtful interest.

NBS is the most suited and flexible tool to this purpose, because it provides a wide mapping of the full dispersion curves of such motions, that can only be detected in the first Brillouin zone, due to the non-crystalline nature of the samples and the

consequently fast damping of the modes with increasing Q-values. In addition, the combination with polarisation analysis can make NERTHUS the elective instrument for studying these phenomena, because it allows the measurement of both coherent and incoherent dynamics, thus achieving a complete picture for such hydrogenated systems.

2.1.4 Collective Dynamics of Liquid Crystals

A significantly emerging science case in recent years is the study of collective dynamics in liquid crystals, which, due to the non-crystalline and mesoscopic nature of the samples, mostly occurs in the first Brillouin zone. For this reason, its experimental investigation represents a significant challenge for current spectroscopic techniques. For instance, by means of inelastic X-ray scattering (IXS), mesogenic liquids crystals in the smectic phase were shown to support both acoustic and optical phonons, the latter being tentatively ascribed to out-of-phase molecular tilts of the aligned liquid crystals [55]. Unambiguously resolving these modes is technically demanding: IXS often lacks the energy resolution – typically limited to 1-1.5 meV – required to clearly distinguish between the transverse acoustic, longitudinal acoustic, and optical branches. On the other hand, traditional inelastic neutron scattering suffers from kinematic restrictions and requires deuteration of the samples to suppress the otherwise dominant incoherent excitations. Furthermore, IXS carries a risk of beam-induced damage to delicate organic samples. With its design optimised for NBS measurements, NERTHUS would overcome these limitations by providing superior resolution at low Q, where it can clearly resolve all the phonon contributions across varying energy settings. Moreover, the combination with polarisation analysis would allow the separation of incoherent contributions, thus providing clean access to the coherent modes of interest. This detailed level of information is essential for understanding how molecular conformations can be tuned via temperature- or field-induced transitions, ultimately enabling the engineering of optically active crystals with tailored vibrational properties.

2.1.5 Magnetic Excitations

Ferromagnetic spin waves from polycrystalline samples are traditionally very hard to measure with inelastic neutron scattering because of neutron kinematic relations restricting the measurable region in $Q - E$ space at the low wavevector- and relatively high energy transfer side. However, this is precisely where the powder averaged excitations of dominantly ferromagnetic systems lie. Studying those systems has recently re-gained a lot of interest as many anisotropic magnets show complex- and frustrated magnetic excitations even if dominantly ferromagnetic. A prime example the Kitaev model on the honeycomb lattice that has a spin-liquid ground state for both ferromagnetic and anti-ferromagnetic Kitaev couplings [56].

NERTHUS with a minimal scattering angle of about 1° will enable to probe the region in $Q - E$ space necessary to determine the magnetic Hamiltonians describing these systems. Especially in novel materials where the community has managed to synthesize powder samples but the routes to single crystals have not yet been discovered. Having detectors up to a maximum $2\Theta = 120^\circ$ will enable us to measure a wide enough dispersion relation of magnetic excitations to refine models further and potentially measure effects of magnon-phonon coupling. The proposed E_i range of approximately 20 to 200 meV is sufficient to cover a wide range of interesting magnetic materials, predominately containing transition metal magnetic elements that fall into this energy range. The relatively high elastic energy resolution of $\Delta E/E = 3\%$ will be especially important if using a higher E_i to measure a lower energy transfer excitations, often necessary to further increase the low Q detection limit at the desired energy transfer (see for example [57]).

2.1.6 Molecular Spectroscopy

Direct-geometry neutron spectrometers have become a routine and indispensable tool for catalysis and molecular spectroscopy experiments, owing to their ability to probe hydrogen dynamics over a broad range of length and time scales. A key strength of direct-geometry instruments is their access to a wide range of Q, enabled by extensive detector coverage, which allows the Q-dependence of dynamical modes to be measured within a single experiment. The key difference between direct- and indirect-geometry spectrometers is that the former can access a much larger Q range and, crucially, can always reach small-Q values. This provides strong complementarity to vibrational spectrometers, which primarily deliver high-energy-resolution information at limited or specific Q values.

Together, direct-geometry and vibrational spectrometers are essential to obtain a complete picture of hydrogen dynamics in catalytic systems, linking vibrational excitations with their spatial and dynamical characteristics. NERTHUS will offer access to shorter neutron wavelengths that T-REX is not optimised for.

A few examples of science cases where NERTHUS would be of great value are in the areas of catalysis and gas storage and separation.

Catalysis. The transfer of hydrogen between reagents and products is the main interest. NERTHUS is ideally suited to such studies, enabling high-quality spectroscopic data to be collected from the same sample over a wide energy range. Access to the C–H, N–H, and O–H stretching regions provides a straightforward and robust means of identifying and quantifying surface species, while the fingerprint region, between 0 and 250 meV, contains key information on catalyst–adsorbate interactions. These surface species are often present at low concentrations, such that sensitivity is as critical as energy resolution. NERTHUS is expected to deliver approximately twelve times higher neutron flux than T-REX in the wavelength range of interest, providing a substantial gain in sensitivity and enabling routine measurements of dilute surface species. This enhanced performance will also allow neutron spectroscopic studies of industrially important non-hydrogenous adsorbates, such as CO_x, NO_x, and SO_x, which are currently at or beyond the sensitivity limits of existing instruments [58, 59].

Gas storage and separation. Gas absorption, particularly for CO_2 capture from waste streams, is an area of growing scientific and industrial importance [60]. Previous neutron spectroscopy studies have demonstrated that changes induced by CO_2 or SO_2 adsorption can be detected, but often at the sensitivity limits of existing instruments [58, 59]. The substantially increased short-wavelength flux of NERTHUS could enable systematic investigations of adsorption mechanisms, host–guest interactions, and structural responses in gas-separation materials under realistic conditions.

2.2 Potential societal relevance of the science case

2.2.1 Life science

NERTHUS will provide insights into the collective dynamics of biomolecules, where coherent excitations play a role in biological function. This can impact pharmaceuticals and drug design, where optimising the molecular environment can improve drug delivery and extend the shelf life of temperature-sensitive medications.

2.2.2 Liquids and glasses

Understanding the collective dynamics in disordered materials can help to connect the microscopic disorder to macroscopic properties such as mechanical stability, thermal transport, and acoustic damping. This knowledge can support the development of improved glasses, polymers, and complex fluids used in industrial processes and advanced materials.

2.2.3 Energy materials.

NERTHUS has the potential to provide new detailed and quantitative information on a vast range of materials connected to the transition to an efficient and sustainable carbon-free energy economy, encompassing next generation nuclear fission and fusion reactors, concentrated solar power, industrial waste heat recovery, and advanced batteries and fuel cells.

2.2.4 Catalysis and gas absorption.

By revealing the hydrogen dynamics and gas–host interactions at the atomic scale under realistic conditions, NERTHUS can help elucidate the mechanisms governing catalysis and gas sorption, thus guiding the development of more efficient catalysts for clean fuels and fertilisers, as well as materials for selective CO_2 and SO_x capture. Such advances can reduce industrial energy consumption, improve air quality, and support the transition of captured carbon into valuable products, hence contributing to environmental sustainability and a circular economy.

2.2.5 Magnetic excitations.

Ferromagnetic qubits are a relatively unexplored class of quantum bits that incorporate ferromagnetic materials into superconducting Josephson junctions to control or create quantum states using their magnetic nature. This allows for a higher density and faster operation without the need of external magnetic field. One issue they currently phase is however the shorter coherence times compared to regular Josephson junctions partly due to magnetic quasiparticle excitations in the ferromagnetic material [61]. Inelastic neutron scattering at small scattering angles is the technique needed to understand those quasiparticle excitations and how they can potentially be controlled. Those Ferromagnetic qubits are a promising merger of traditional spintronics and superconductivity to create compact and scalable quantum computing hardware. Ferromagnetic materials like the ones to be studied on NERTHUS are fundamental as sources, manipulators, and detectors of spin-polarised currents in spintronics.

Especially 2D ferromagnets drive the advancement in non-volatile, high-speed, and low-power devices [62]. The high-speed directly stems from the more compact devices possible using 2D ferromagnets but inelastic neutron scattering is needed to understand the microscopic magnetic interaction in those materials before they can be used in any devices.

2.3 Potential new science

NERTHUS will provide so-far unavailable possibilities to combine NBS with polarisation analysis, together with high flux and low background. A number of science cases exist that can greatly benefit from these characteristics, or that could not be properly tackled at all until now, that range from 2D magnetism to the fundamental physics of liquids and glasses, from drug design to energy materials. Therefore, we envisage that NERTHUS will unlock many new possibilities within and beyond the science cases outlined in section 2.1 and, more generally, for samples available in limited quantities.

2.4 Potential user community

NERTHUS has the potential to support a wide range of interdisciplinary research across condensed matter physics, materials science, energy-related materials, magnetism and biophysics, besides the more traditional field of liquids and glasses. Overall, a host of scientific subjects where the microscopic dynamics of non-crystalline materials, which are widely spread in Nature, has lacked the possibility of being studied in the most appropriated dynamical region. Moreover, specific scientific cases, such as phase transitions in liquid crystals, could also attract researchers traditionally working with X-ray scattering to neutron techniques.

3 AN INITIAL TECHNICAL OVERVIEW OF THE PROPOSED INSTRUMENT, DISCUSSING TECHNICAL FEASIBILITY

NERTHUS will be a direct geometry thermal spectrometer based on a new implementation of the time-focusing technique that disentangles wavelength and beam-divergence [63]. The key element is a double rotating-crystal monochromator (DRCM) that is used to extract from a wide wavelength band from the white beam [64]. The time-focusing allows to achieve a good resolution whereas the double crystal setup transports the original beam collimation to the monochromatic beam [64]. A schematic view of the working principle is shown in the inset of Fig. 1. Incident wavelength and resolution can be tuned by the rotation speed and the relative position of the DRCM elements, whereas their phasing eliminates unwanted harmonics. In addition, the DRCM shifts the monochromatic beam away from the primary one, thus avoiding the direct view of the source with a significant background reduction.

Figure 1 shows a possible layout of NERTHUS. The first part of the spectrometer is the transport optics. As already mentioned, the DRCM separates the monochromatic beam from the primary one. Consequently, the instrument can be short with a straight guide. Moreover, the crystal monochromator accepts a limited divergence, hence the guide can have a relatively low m-value ($m = 4$). The DRCM is contained in a chamber where the rotating elements M1 and M2 can translate to set the appropriate Bragg angle θ_M and the time-focusing distance. The dimension of the DRCM chamber limits the accessible wavelengths and resolutions. In the following, a length of 1.5 m is considered. The last portion of the primary spectrometer includes a 1 m exchangeable guide and the sample chamber. Possible interchangeable components are:

(i) a low-divergence collimator for small-angle experiments;
(ii) a converging guide element for small samples;
(iii) a supermirror polarising guide for polarisation measurements.

The sample chamber is a cylinder with dimensions according to the ESS specifications, to ensure compatibility with common sample environment devices and a ^{3}He cell analyser for polarisation analysis. The primary spectrometer flight path is under vacuum. Single-crystal silicon windows, which present negligible beam attenuation off Bragg scattering, can be used to effectively separate different portions of the beam line when needed. The last component of the instrument is the large-area position-sensitive detector with a sample-to-detector distance $L_{SD} = 4$ m with an ideal angular coverage from -10° to 135°. The detector must be optmised for thermal neutrons and can share the same technology used for T-REX, i.e. the boron-10 based Multi-Grid detector. It is worth noting that small-angle experiments require only limited angular coverage, ideally from -10° to 15°.

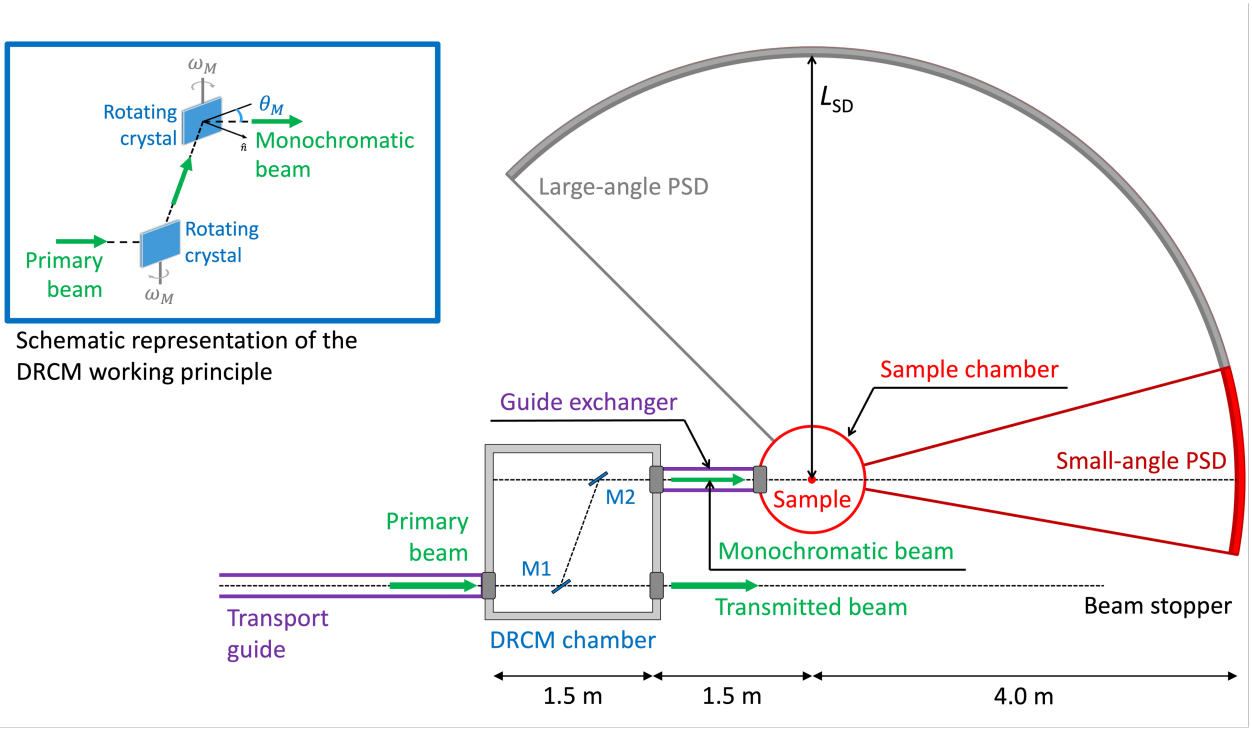

Figure 1. Layout of NERTHUS with a single DRCM. The first part of the beamline, from the source to the DRCM chamber is omitted for clarity sake. The red portion of the detector is the small-angle option. Inset: schematic rappresentation of the DRCM working. To achieve the time focusing for the selected wavelength band, the crystals M1 and M2 are rotated with a proper direction (black circular arrows), angular velocity ω_M and phase (not drawn). The Bragg angle θ_M is defined as the angle between the crystal surface and the incoming/outgoing beam; $\hat{n}$ is the unit vector indicating the direction perpendicular to the crystal surface.

3.1 Estimated performances

NERTHUS performances are mainly defined by the choice of the DRCM crystals, in particular the plane distance d, the reflection order n, the mosaicity Δ_i and the peak reflectivity R_i. The first possible option is highly oriented pyrolytic graphite (HOPG) that provides a high peak reflectivity even at relatively short wavelengths (e.g. $R_i \simeq 0.7$ at about 1.3 Å, see Ref. [65]). Moreover, the peak reflectivity shows a minor dependence as a function of the reflection order when employed in the symmetric reflection configuration. High reflectivity is crucial to minimize intensity losses due to the double monochromator configuration and HOPG produces a clean reflected beam and no spurious components due to multiple reflections. Using the (002) reflection and its high order multiples, we can span the wavelength range down to $\lambda_i \simeq 1$ Å. Conversely, the shorter wavelengths require different materials such as copper or germanium.

We analyse the performance of the spectrometer described in Fig. 1 and based on a DRCM with different crystals. We can thus estimate its potential performances in terms of wavelength and energy resolution, by comparing the useful flux with that expected for an equivalent chopper spectrometer. Of course, an absolute evaluation of the flux at the sample would require a detailed simulation of the neutron source and the primary neutron transport system, which is far beyond the purpose of this work.

Once defined the monochromator, the reflection order, the choice of the desired wavelength λ_i defines the Bragg angle θ_M and the relative position of the two monochromators. The time-focusing distance $L_M D$ is thus defined as:

$$L_{MD} = v_i \frac{\tan\theta_M}{\omega_M} \tag{1}$$

where v_i is the velocity of the neutrons with λ_i and ω_M the monochromator angular speed. The latter has to be coupled to the source frequency and is then limited to a multiple of the source frequency ν_s. Considering the dimensions in Fig. 1, the time-focusing distance L_{MD} can vary between 5.5 m and 7.5 m. Table 1 shows some possible combinations of parameters that match the constraints of the proposed layout.

The last two columns in Tab. 1 shows the relative elastic resolution $\Delta E_i/E_i$ and the gain factor G with respect to a equivalent

crystal	n	λ_i (Å)	E_i (meV)	θ_M (°)	ν_M (Hz)	$\Delta E_i/E_i$ (%)	G
Cu(220)	2	0.80	127.81	38.75	105	2.0	21.0
Cu(220)	2	0.90	100.99	44.77	105	2.0	21.6
Ge(355)	2	0.80	127.81	47.05	147	3.1	12.9
Ge(355)	2	0.90	100.99	55.43	147	2.9	12.1
HOPG(002)	4	1.00	81.80	36.61	84	3.3	12.4
HOPG(002)	3	1.50	36.36	42.13	63	3.0	12.9
HOPG(002)	2	2.00	20.45	36.61	42	3.3	12.4

Table 1. Possible instrument configurations based on the design shown in Fig. 1. The elastic energy resolution $\Delta E_i/E_i$ and the gain factor G with respect to a chopper instrument are calculated using the formulas in [63].

chopper spectrometer. The energy resolution ΔE_i is calculated according to the analytical formulae in Ref. [63]. Conversely the gain factor G is calculated with respect to a chopper spectrometer with similar performance, see Ref. [63]. In particular, we consider only the main term given by the ratio between the DRCM opening time and the chopper one. Other terms are due to the different beam size and crystal reflectivity and compensates. This rough but effective calculation is a conservative estimation that does not account for differences in the primary transport beam that add a further gain factor in favour of NERTHUS. Indeed, the losses due to its short, straight neutron guide are lower than those due to the long S-shaped ones of chopper spectrometer at ESS. The estimation was banchmarked against ray-tracing simulations and complete MCSTAS analysis of the NERTHUS beamline is under developement.

The signal-to-noise ratio of an instrument is one of the key figure-of-merit to define its quality. However, a reliable estimate of the background of a neutron spectrometer is a complex task that requires a specialization of source and instrument design that goes well beyond the scope of this proposal. Even so, some general and qualitative comments can be made. Due to the intrinsic geometry of a DRCM, the monochromatic beam is moved away from the primary beam, so that the sample and detector are never in direct sight of the neutron source, see Fig. 1. This is expected to result in a significant background drop. A further background source is the environmental noise due to the presence of other instruments (e.g. cross-feeding among neutron guides). This is common to every instrument in every facility and can be reduced only using a proper shielding. However, it is worth noting that the proposed instrument is rather short and this significantly eases the requirements for an effective shielding.

3.2 Possible problems and mitigation

The innovative component of the proposed instrument is the double rotating-crystal monochromator. In order to maximize both flux and versatility, the DRCM has to cover a wide area with a tunable rotating frequency up to about 100 Hz. However, to avoid the mechanical difficulties connected with the rotation of a large-surface device, the DRCM can be built with a set of smaller rotating elements, each containing a subset of small crystals conveniently held and aligned by a proper mechanical support. The crystal holder is a 2 cm diameter cylinder composed by two symmetric halves, where slab-shaped crystals lay on the cylinder axis. The sample holder can be done in aluminum and most of the inner material can be removed until the external wall is reduced to less than 1 mm. Consequently, neutron attenuation and background due to scattering by the supports are strongly reduced, while the necessary mechanical stability is preserved. A suitable number of such cylindrical elements can be easily disposed next to each other with parallel vertical axes, to cover the desired total monochromator area. Figure 2 shows a working prototype of this element. The small radius of the cylinders significantly lowers the peripheral speed of the crystal edges with respect to a wholly rotating crystal, thus making rotational forces and Doppler effects on the speed of the diffracted neutrons negligible. A rotation frequency of about 100 Hz implies a peripheral speed of about 7 m/s, wich is neglegible when compared to the velocity of thermal neutron in the selected range. A prototype of this device has been built and extensively tested [64]. In particular, a long term rotation test has shown no mechanical failures over a several months of operation at 100 Hz.

The proposed time-focusing approach can be implemented in two alternative ways that do not require or limit the number of rotating elements:

(i) with two sets of static crystal monochromators;
(ii) with a single rotating monochromator plus a cascade of static ones.

In the first case, each monochromator is obtained as a cascade of static crystals whose Bragg angle θ_M is slightly rotated to extend the extracted wavelength band and extract fast neutrons at longer distances than to slow ones thus achieving the time-focusing at

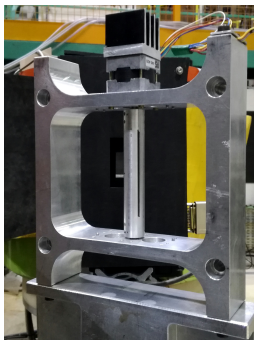

Figure 2. Prototype of a DRCM element during a test at the IN3 beamline (Institut Laue Langevin, Grenoble). The thin 2mm edge of the HOPG crystals appears as a vertical black line along cylinder. composed of three rotating elements.

the detector positions. The two monochromators are parallel and placed at a convenient distance L_{1-2}. This setup is cumbersome and does not prevent the presence of high-order contaminations in the monochromatic beam. Consequently, this setup requires the presence of a chopper on the monochromatic beam to get rid of unwanted harmonics and define the time structure for ToF analysis. In the second setup, the role of the chopper is done by a rotating crystal that reflects neutron to properly oriented static crystals. In this case, the chopper is still needed to reject the unwanted wavelenghts. Both the setups are cumbersome and limits the number of monochromating elements. On the other hand, unwanted harmonics can be used for doing experiments at diffent wavelengths.

It is worth noting that DRCMs offer a versatile solution with no technological issues. The static-static and rotating-static options can be also investigated as risk mitigation possibilities. These alternatives are under study with further specific simulations. Final evaluations with a complete risk analysis will be done by the ESS constructing team.

4 AN EXPLANATION OF HOW THE CONCEPT MAKES USE OF THE ESS LONG-PULSE SOURCE, IF RELEVANT

For long-pulse and continuous sources, the performances can be enhanced over the thermal and cold-neutron ranges, using hybrid spectrometers exploiting the time-focusing technique. This approach consists in selecting a broader portion of the white beam in such a way that neutrons of different velocities reach the detector at the same time. Compared with standard chopper instruments, this configuration uses a longer extraction time, which provides a higher flux at the sample. However, the typical implementation of the time-focusing technique exploits an increased beam divergence to broaden the band of accepted wavelengths, therefore the flux gain is counterbalanced by a poorer Q-resolution. Examples of direct geometry instruments employing time-focusing are IN4/PANTHER and IN6/SHARPER at ILL, and FOCUS at PSI.

5 PLANS OR REQUIREMENTS FOR SAMPLE ENVIRONMENT AND LABORATORY ACCESS

The instrument can benefit from the access to the several laboratories at the ESS for sample preparation and complementary characterisation. Depending on the final location of the instrument, several options are possible in D04, D08 or E04. The users can also profit from the different ancillary equipment offered by the ESS laboratories such as Xray diffraction (powder and single crystal), FTIR, Raman, Laue camera for single crystal alignment, DLS, calorimetry, UV/VIS spectrometer, Xray fluorescence, ICP-OES etc.

The NERTHUS sample environment area will be designed to accommodate the diverse requirements of different scientific communities. An initial sample environment suite will include:

- Cryofurnace: Temperature range: 2–800 K, routine sample environment for all scientific cases that need low temperature in the range of a few K and/or large temperature range.
- Rotation stage, for single crystals.
- Access to high temperature furnace, temperature range: 300 –1300 K for scientific cases that require high temperatures beyond standard cryofurnace, e.g., dynamics of inorganic glasses, energy materials.
- Access to high-pressure systems (Paris-Edinburgh cells, liquid pressure cells, gas pressure cells) and gas sorption equipment.

The requirement for sample environment is to be non-magnetic (magnetic permeability $\mu \leq 1.01$) to be compatible with polarisation analysis. The requirement also applies to other ESS spectrometers (e.g. TREX and CSPEC), thus NERTHUS can exchange equipment with other spectrometers and rely on previously acquired knowledge at the ESS.

6 PROPOSED LOCATION OF THE INSTRUMENT AT THE ESS FACILITY INCLUDING MOTIVATION

NERTHUS is a compact instrument, thus in principle it could fit in length at any available beamport in D01 or D03. However, to maximise the thermal neutron extraction, central ports with respect to the moderator are preferable. To also accommodate the large detector option, beamport E8 seems the most suitable one, considering all factors. Moreover, with some adaptations, NERTHUS could also be considered as a symbiotic instrument for NJORD.

7 GAP ANALYSIS IN TERMS OF BOTH CAPABILITY AND CAPACITY, IN RELATION TO ESS AND THE GLOBAL FACILITY LANDSCAPE

7.1 Gap analysis: Capacity/Capability

Currently, there are no dedicated NBS instruments, hence NERTHUS would cover a capability gap existing not only at the ESS but in the entire neutron community. By exploiting the unique long pulse of the ESS source, it will offer access to the first (pseudo) Brillouin zone with settings never explored before, such as the combination with polarisation analysis and unprecedent flux and low background.

Moreover, with the large detector option, NERTHUS will add at the ESS both capacity and capabilities in the thermal incident energy regime, with its complementary coverage of the dynamical range, with respect to other thermal instruments of the facility. For instance, while T-REX accesses the thermal regime, its incident flux drops significantly at energies above 100–120 meV due to its curved neutron guide design and length, leaving a number of experiments impossible to perform within the current suite of direct geometry instruments. VESPA provides access to high incident energies and flux, but its detector geometry restricts access to specific points within the energy and momentum transfer spaces, unlike the continuous detector coverage possible with direct geometry instruments. Therefore, in addition to allowing NBS experiments, NERTHUS would effectively bridge the gap between VESPA and TREX, enabling high-flux measurements at elevated incident energies and extending coverage in (Q, E)-space.

8 COMPARISON TO OTHER SIMILAR INSTRUMENTS IN THE WORLD, IF POSSIBLE

At present there exist no other neutron spectrometer capable of efficiently performing NBS measurements, i.e. of accessing the peculiar dynamical range of the first Brillouin zone in non-crystalline systems. The only and ever existed dedicated instrument, BRISP at the ILL, suffered from a high background because of its unpractical location on top of a steel platform in the ILL reactor hall, which seriously limited shielding options. Other previous or existing thermal instruments are general-purpose spectrometers that offer NBS as a special configuration only. Examples are the old IN4C at the ILL and HRC at J-PARC. These non-dedicated spectrometers are always underperforming in the first Brillouin zone, mainly because they need to trade off collimation for flux, in order to be safely competitive in the traditional wide-scattering-angle region. As a consequence, NBS experiments, that instead need a clean access to thermal exchanged energies at small angles, have never enjoyed a dedicated and optimised instrument. Thanks to the combination of the double monochromator with the unique long pulse of ESS, for the first time NERTHUS can provide both an efficient access to NBS and a good complementary access to traditional wide-angle spectroscopy.

REFERENCES

(1) Zanatta, M.; Sacchetti, F.; Guarini, E.; Orecchini, A.; Paciaroni, A.; Sani, L.; Petrillo, C. *Phys. Rev. Lett.* **2015**, *114*, 187801.
(2) Zanatta, M.; Orecchini, A.; Sacchetti, F.; Petrillo, C. *Journal of Molecular Liquids* **2024**, *393*, 123550.
(3) Petrillo, C.; Sacchetti, F. *Advances in Physics: X* **2021**, *6*, 1871862.
(4) Baldi, G.; Fontana, A.; Monaco, G. In *Low-Temperature Thermal and Vibrational Properties of Disordered Solids*, 2022; Chapter Chapter 6, pp 177–226.
(5) Singh, S.; Ediger, M.; De Pablo, J. J. *Nature Materials* **2013**, *12*, 139–144.

(6) Ràfols-Ribé, J.; Will, P.-A.; Hänisch, C.; Gonzalez-Silveira, M.; Lenk, S.; Rodríguez-Viejo, J.; Reineke, S. *Science Advances* **2018**, *4*.
(7) Wang, L.; Ninarello, A.; Guan, P.; Berthier, L.; Szamel, G.; Flenner, E. *Nature Communications* **2019**, *10*.
(8) Janek, J.; Zeier, W. G. *Nature Energy* **2016**, *1*, 16141.
(9) Ahammed, B.; Ertekin, E. *Advanced Materials* **2024**, *36*.
(10) Joshi, A.; Mishra, D. K.; Singh, R.; Zhang, J.; Ding, Y. *Applied Energy* **2025**.
(11) Shang, R.; Ma, Y.; Anduaga-Quiros, K.; Briseno, G.; Ning, Y.; Chang, H.-J.; Ozkan, M.; Ozkan, C. S. *Nanomaterials* **2025**, *15*.
(12) Muy, S.; Schlem, R.; Shao-horn, Y.; Zeier, W. *Advanced Energy Materials* **2020**, *11*.
(13) Sau, K.; Takagi, S.; Ikeshoji, T.; Kisu, K.; Sato, R.; dos Santos, E. C.; Li, H.; Mohtadi, R.; Orimo, S.-i. *Communications Materials* **2024**, *5*, 122.
(14) Gupta, M. K.; Ding, J.; Lin, H.-M.; Hood, Z. D.; Osti, N.; Abernathy, D.; Yakovenko, A.; Wang, H.; Delaire, O. *Chemistry of Materials* **2024**.
(15) Gupta, M.; Ding, J.; Bansal, D.; Abernathy, D.; Ehlers, G.; Osti, N.; Zeier, W.; Delaire, O. *Advanced Energy Materials* **2022**, *12*.
(16) Brenner, T. M.; Grumet, M.; Till, P.; Asher, M.; Zeier, W. G.; Egger, D. A.; Yaffe, O. *The Journal of Physical Chemistry Letters* **2022**, *13*, 5938–5945.
(17) Gupta, M. K.; Ding, J.; Osti, N. C.; Abernathy, D. L.; Arnold, W.; Wang, H.; Hood, Z.; Delaire, O. *Energy Environ. Sci.* **2021**, *14*, 6554–6563.
(18) Ding, J.; Gupta, M. K.; Rosenbach, C.; Lin, H.-M.; Osti, N. C.; Abernathy, D. L.; Zeier, W. G.; Delaire, O. *Nature Physics* **2025**, *21*, 118–125.
(19) Aghoghovbia, O.; Rurali, R.; Al-fahdi, M.; Ojih, J.; Jiang, D.-e.; Hu, M. *Materials horizons* **2025**.
(20) Ren, Q. et al. *Nature Materials* **2023**, *22*, 999–1006.
(21) Shen, X.; Koza, M.; Tung, Y.-H.; Ouyang, N.; Yang, C.-C.; Wang, C.; Chen, Y.; Willa, K.; Heid, R.; Zhou, X.; Weber, F. *Small* **2023**, e2305048.
(22) Novak, E.; Daemen, L.; Jalarvo, N. *Materials* **2024**, *17*.
(23) Bhatnagar, P.; Siddiqui, S.; Sreedhar, I.; Parameshwaran, R. *International Journal of Energy Research* **2022**, *46*, 17755–17785.
(24) Cui, K.; Zhao, W.; Li, S.; Zhou, D.; Liu, C.; Qu, X.; Li, P. *ACS Sustainable Chemistry & Engineering* **2022**, *10*, 1871–1879.
(25) Zhao, A. Z.; Garay, J. *Progress in Materials Science* **2023**.
(26) Niedermeier, K. *Energy Storage* **2023**, *5*.
(27) Kondaiah, P.; Pitchumani, R. *Renewable Energy* **2023**, *205*, 956–991.
(28) Zhang, S.; Liu, Y.; Fan, Q.; Zhang, C.; Zhou, T.; Kalantar-zadeh, K.; Guo, Z. *Energy and Environmental Science* **2021**.
(29) Kondo, M. *IOP Conference Series: Earth and Environmental Science* **2019**, *364*, 012012.
(30) Forsberg, C.; Zheng, G. (; Ballinger, R. G.; Lam, S. T. *Nuclear Technology* **2020**, *206*, 1778–1801.
(31) Cockrell, C.; Withington, M.; Devereux, H. L.; Elena, A. M.; Todorov, I. T.; Liu, Z. K.; Shang, S. L.; McCloy, J. S.; Bingham, P. A.; Trachenko, K. *The Journal of Physical Chemistry B* **2025**, *129*, 2271–2279.
(32) Zhao, A. Z.; Wingert, M. C.; Chen, R.; Garay, J. E. *Journal of Applied Physics* **2021**, *129*, 235101.
(33) Guarini, E.; Francesco, A. D.; Bafile, U.; Laloni, A.; del Rio, B. G.; González, D.; González, L.; Barocchi, F.; Formisano, F. *Physical Review B* **2020**.
(34) Price, D. L.; Copley, J. *Physical Review A* **1975**, *11*, 2124–2133.
(35) Petrillo, C.; Sacchetti, F. *Advances in Physics: X* **2021**, *6*.
(36) Voneshen, D.; Stewart, J.; Ewings, R. *Nuclear Instruments and Methods in Physics Research Section A: Accelerators, Spectrometers, Detectors and Associated Equipment* **2023**, *1052*, 168289.
(37) Ghosh, T.; Dutta, M.; Sarkar, D.; Biswas, K. *Journal of the American Chemical Society* **2022**.
(38) Dutta, M.; Sarkar, D.; Biswas, K. *Chemical communications* **2021**.
(39) Zhu, J.; Shen, X.; Ma, J.; Ding, J. *The Innovation Energy* **2024**.
(40) Taneja, V.; Das, S.; Dolui, K.; Ghosh, T.; Bhui, A.; Bhat, U.; Kedia, D. K.; Pal, K.; Datta, R.; Biswas, K. *Advanced Materials* **2023**, *36*.
(41) Zeng, Z.; Zhang, C.; Yu, H.; Li, W.; Pei, Y.; Chen, Y. *Materials Today Physics* **2021**, *21*, 100487.
(42) Jen, I.-L.; Lin, C.-Y.; Wang, K.-K.; Wu, C.-M.; Lee, C.-H.; Wu, H.-J. *Advanced Science* **2024**, *12*.

(43) Zhu, Y.; Wei, B.; Liu, J.; Koocher, N. Z.; Li, Y.; Hu, L.; He, W.; Deng, G.; Xu, W.; Wang, X.; Rondinelli, J. M.; Zhao, L.-d.; Snyder, G. J.; Hong, J.-w. *Materials Today Physics* **2021**.
(44) Zhang, J.; Ishikawa, D.; Koza, M. M.; Nishibori, E.; Song, L.; Baron, A. Q.; Iversen, B. B. *Angewandte Chemie* **2023**.
(45) Xu, Y.; Zhou, Y.; Li, Y.; Ding, Z. *Molecules* **2024**, *29*.
(46) Chung, H. W.; Cladek, B.; Hsiau, Y.-Y.; Hu, Y.-Y.; Page, K.; Perry, N. H.; Yildiz, B.; Haile, S. *MRS Bulletin* **2024**, *49*, 435–450.
(47) Mamontov, E.; Kolesnikov, A.; Sampath, S.; Yarger, J. *Scientific Reports* **2017**, *7*.
(48) Rulev, A.; Nagasawa, N.; Wang, H.; Pomjakushin, V.; Kunz, M.; Yoda, Y.; Cramer, S. P.; Chen, Q.; Braun, A. *Advanced Science* **2025**, *13*.
(49) Lynn, J. W.; Huang, Q.; Brown, C. M.; Brown, C. M.; Miller, V.; Foo, M.; Schaak, R.; Jones, C. Y.; Mackey, E.; Cava, R. *Physical Review B* **2003**, *68*, 214516.
(50) Ramirez-Cuesta, A.; Xicohtencatl, R. B.; Cheng, Y. *Journal of Materials Research* **2024**, *39*, 727–736.
(51) Hempelmann, R.; Oxford University Press: 2000.
(52) Turton, D. A.; Senn, H. M.; Harwood, T.; Lapthorn, A. J.; Ellis, E. M.; Wynne, K. *Nature Communications* **2014**, *5*.
(53) Acbas, G.; Niessen, K. A.; Snell, E. H.; Markelz, A. G. *Nature Communications* **2014**, *5*.
(54) Kolossvary, I. *JACS AU* **2024**, *4*, 1303–1309.
(55) Bolmatov, D.; Zhernenkov, M.; Sharpnack, L.; Agra-Kooijman, D. M.; Kumar, S.; Suvorov, A.; Pindak, R.; Cai, Y. Q.; Cunsolo, A. *NANO LETTERS* **2017**, *17*, 3870–3876.
(56) Kitaev, A. *Annals of Physics* **2006**, *321*, 2–111.
(57) Ono, K.; Inami, N.; Saito, K.; Takeichi, Y.; Yano, M.; Shoji, T.; Manabe, A.; Kato, A.; Kaneko, Y.; Kawana, D.; Yokoo, T.; Itoh, S. *Journal of Applied Physics* **2014**, *115*, 17A714.
(58) Yu, X.; Cheng, Y.; Li, Y.; Polo-Garzon, F.; Liu, J.; Mamontov, E.; Li, M.; Lennon, D.; Parker, S. F.; Ramirez-Cuesta, A. J., et al. *Chemical Reviews* **2023**, *123*, 8638–8700.
(59) Parker, S.; Lennon, D. *Physchem* **2021**.
(60) Moon, H.; Heller, W. T.; Osti, N.; Song, M.; Proaño, L.; Vaghefi, I.; Jones, C. W. *Industrial & Engineering Chemistry Research* **2024**, *63*, 15100–15112.
(61) Kim, S.; Abdurakhimov, L. V.; Pham, D.; Qiu, W.; Terai, H.; Ashhab, S.; Saito, S.; Yamashita, T.; Semba, K. *Communications Materials* **2024**, *5*, 216.
(62) Nie, T. et al. *Review of Materials Research* **2026**, *2*, 100145.
(63) Zanatta, M.; Andersen, K. H.; Deen, P. P.; Orecchini, A.; Paciaroni, A.; Petrillo, C.; Sacchetti, F. *Review of Scientific Instruments* **2019**, *90*, 095101.
(64) Zanatta, M.; Orecchini, A.; Aisa, S.; Casinini, F.; Farnesini, L.; Deen, P. P.; Paciaroni, A.; Petrillo, C.; Sacchetti, F. *J. Phys.: Conf. Ser.* **2016**, *746*, 012002.
(65) Riste, T.; Otnes, K. *Nuclear Instruments and Methods* **1969**, *75*, 197–202.